



The Impact of the Core's Material on the Absorption of a Quantum Dot–Metal Nanoshell Hybrid System [†]

Alexandros Kontakos, Emmanuel Paspalakis  and Spyridon G. Kosionis * 

Materials Science Department, School of Natural Sciences, University of Patras, 265 04 Patras, Greece

* Correspondence: kosionis@upatras.gr; Tel.: +30-2610-996315

[†] Presented at the 3rd International Electronic Conference on Applied Sciences, 1–15 December 2022; Available online: <https://asec2022.sciforum.net/>.

Abstract: In this study, we investigate the linear optical response in a hybrid nanostructure composed of a semiconductor quantum dot and a metal shell nanoparticle. We analyze a case wherein the nanostructure interacts with an incident electromagnetic field with polarization parallel to the symmetry axis of the nanosystem. We derive nonlinear density matrix equations in the rotating wave approximation under the quasistatic response of the system, and use a series expansion method to obtain analytical functions for linear susceptibility with respect to both components of the nanostructure. The imaginary part of these expressions is related to the absorption coefficient. We investigate the way in which the modification of the core's material affects the characteristics of the spectral resonance. For low values of the dielectric constant, the system exhibits amplified gain without population inversion and quenched absorption resonance, while for high values of the dielectric constant, we observe suppression of the gain dip and enhancement of the absorption resonance. In the first regime, the exciton lifetime is suppressed, and in the second case, its value is importantly increased, especially in the case of small interparticle distances where the semiconductor quantum dot and metal shell nanoparticle interact strongly.

Keywords: absorption; gain; hybrid nanostructure; metal nanoshell; semiconductor quantum dot

Citation: Kontakos, A.; Paspalakis, E.; Kosionis, S.G. The Impact of the Core's Material on the Absorption of a Quantum Dot–Metal Nanoshell Hybrid System. *Eng. Proc.* **2023**, *31*, 82. <https://doi.org/10.3390/ASEC2022-13805>

Academic Editor: Nunzio Cennamo

Published: 2 December 2022

Publisher's Note: MDPI stays neutral with regard to jurisdictional claims in published maps and institutional affiliations.



Copyright: © 2022 by the authors. Licensee MDPI, Basel, Switzerland. This article is an open access article distributed under the terms and conditions of the Creative Commons Attribution (CC BY) license (<https://creativecommons.org/licenses/by/4.0/>).

1. Introduction

During the last two decades, hybrid nanostructures fabricated by coupling semiconductor quantum dots (SQDs) with metal nanoparticles have attracted scientific interest [1–12], since they produce unique optical effects. These novel properties owe their presence to the creation of hybrid excitons originating from the long-range Coulomb coupling between excitons and plasmons, and have been extensively investigated in systems where a metal nanosphere is coupled to an SQD [1–10]. However, the use of metal nanoparticles with a more complex structure may give rise to a series of interesting optical phenomena, making such systems ideal candidates for applications in the field of nanophotonics. For instance, the coupling of a metal nanoshell (MNS) with a dielectric core to an SQD provides the advantage of tuning the optical properties of the system more efficiently, by properly adjusting the size and the material of the core [11,12].

In the present work, we aim to explore the novel characteristics that may arise on the absorption spectrum of both the SQD and the MNS in a hybrid system where these two components are coupled together, by properly adjusting the dielectric constant of the core material. We first derive the equations of motion in the rotating wave approximation, and expand the density matrix elements in the first order with respect to the incident field. The multipolar polarizability regime is applied [4,10–12], which provides a more accurate description of the interaction between the SQD and the nanoshell. After solving the equations in the steady state, we obtain analytical expressions for the calculation of the positions and the amplitudes of the maxima and the minima detected on the absorption spectrum, as well as of the full width at half maximum (FWHM) of the absorption resonance.

2. Methods

The hybrid nanosystem consists of an MNS structure and an SQD, and is placed in a dielectric medium, as illustrated in Figure 1. The dielectric constants of the environment and the SQD are denoted as ϵ_{env} and ϵ_s , respectively. The MNS structure is composed of a dielectric core with a radius r_1 and a gold metal nanoshell with an outer radius r_2 , and dielectric function $\epsilon(\omega)$. The core is made of a material with a dielectric constant ϵ_c . The center-to-center distance between the nanoparticles is R . We model the SQD as a two-level system, with E_0 and E_1 being the energies of the ground state $|0\rangle$ and the excited state $|1\rangle$, respectively, with energy difference $\hbar\omega_{01} = E_1 - E_0$.

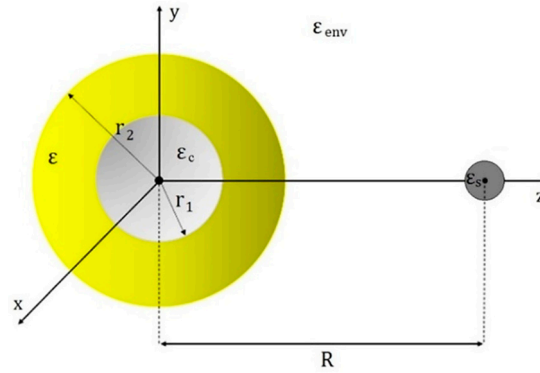


Figure 1. Schematic configuration of the hybrid system.

The entire hybrid system is subjected to an external classical electromagnetic field $E(t) = E_0 e^{-i\omega t} + c.c$, which excites the interband transition $|0\rangle \rightarrow |1\rangle$. The Hamiltonian that governs the population dynamics of the SQD, in the dipole approximation, is:

$$H = \hbar\omega_{01}|1\rangle\langle 1| - \hbar\left[(\Omega + G\sigma_{10})e^{-i\omega t} + c.c.\right](|0\rangle\langle 1| + |1\rangle\langle 0|), \quad (1)$$

where we also introduce the following two key parameters:

$$\Omega = \frac{E_0\mu}{2\hbar\epsilon_{effs}} \left(1 + \frac{s_{pol}f_1(\omega)r_2^3}{R^3}\right) = \Omega_R + i\Omega_I, \quad (2)$$

$$G = \frac{\mu^2}{4\pi\hbar\epsilon_0\epsilon_{effs}^2\epsilon_{env}} \sum_{n=1}^{10} \frac{(n+1)^2 f_n(\omega)r_2^{2n+1}}{R^{2n+4}} = G_R + iG_I. \quad (3)$$

The first and the second terms of the Rabi frequency Ω are, respectively, associated with the coupling of the SQD with the probe electric field and the field emitted by the MNS, due to the induction of polarization [8]. The G parameter is related to the self-interaction of the SQD. The ϵ_{effs} factor accounts for the screening of the SQD [10]. The definition of the first-order polarizability of a core-shell nanoparticle is $\alpha_1(\omega) = 4\pi r_2^3 f_1(\omega)$, with $f_1(\omega) = f_{1R} + if_{1I}$ being a complex factor given in Ref. [12]. In the multipole expansion approach, the polarizability factor is defined as $f_n(\omega)$ [13].

After deriving the density matrix equations and expanding the density matrix elements in the first-order Taylor series, with respect to the amplitude of the weak probe field, we solve the obtained equations in the steady state and calculate the absorption coefficient (imaginary part of the linear susceptibility of the SQD), as in Ref. [10], with the corresponding critical points.

$$\text{Im}[X_{SQD}]_{max/min} = \mp Q \frac{M_I^2}{2(1 + T_2 G_I) \left(\sqrt{M_I^2 + M_R^2} \mp M_R\right)}, \quad (4)$$

where M_R and M_I represent the real and the imaginary parts of the complex factor $M = \frac{1}{\epsilon_{\text{effs}}} \left(1 + \frac{s_{\text{pol}} f_{11}(\omega) T_2^3}{R^3} \right)$, and $Q = -\frac{\Gamma \mu^2 T_2}{\epsilon_0 V \hbar}$ is a negative constant. The position and the FWHM of the absorption resonance are:

$$\delta_{\text{res}} = -G_R - \frac{M_R}{M_I} \left(G_I + \frac{1}{T_2} \right), \text{FWHM} = 2 \sqrt{1 + \frac{M_I^2}{M_R^2} \left(G_I + \frac{1}{T_2} \right)}. \quad (5)$$

Next, we determine the first-order optical susceptibility of the core-shell nanoparticle, as in Ref. [10]. After performing calculations, we derive an analytical expression for the first-order absorption of the MNS:

$$\text{Im}[\chi_{\text{MNS}}] = \frac{3\epsilon_{\text{env}}}{\epsilon_0} f_{11}(\omega) + \Phi \frac{\tilde{M}_I T_2 (\delta + G_R) - \tilde{M}_R (1 + T_2 G_I)}{T_2^2 (\delta + G_R)^2 + (1 + T_2 G_I)^2}. \quad (6)$$

where, $\Phi(R) = -\frac{3s_{\text{pol}} \mu^2 T_2}{4\pi \epsilon_0 \epsilon_{\text{effs}} R^3}$ is an R-dependent quantity, and $\tilde{M} = f_1 \bullet M = \tilde{M}_R + i\tilde{M}_I$ is a complex factor that is frequency-independent, within the short range of frequencies under investigation.

3. Parameters and Results

In this section, we present the profile of the absorption spectrum, as a function of the detuning energy of the applied field from resonance $\hbar\delta = \hbar(\omega - \omega_{01})$, with regard to both the SQD and the MNS. For the calculations, we assume that the MNS is made of gold. The value of the corresponding dielectric function $\epsilon_2(\omega)$ is equal to $(-2.28 + 3.81i)$ [14], for an incident field of energy around 2.5 eV. This value corresponds to the energy that is necessary for the excitation of a localized surface plasmon on the surface of the gold metal nanoshell, and is also equal to the energy band gap of the two-level quantum emitter. The dielectric constant of the environment is $\epsilon_{\text{env}} = 1$ and the dephasing time is $T_2 = 0.3$ ns. The dielectric constant of the semiconductor quantum dot ϵ_s is set equal to 6. and the transition dipole moment is $\mu = 0.65q_e$, where q_e is the electron charge [10]. In the strong confinement regime, we also take $\Gamma/V = 5 \times 10^{23} \text{m}^{-3}$ [15]. We use the multipole polarization regime and maintain terms of up to the order of $N = 10$, as this approximation is sufficient to reach convergence [4]. The MNS is assumed to have a fixed size that is determined by the outer radius, $r_2 = 7.5 \text{nm}$. The radius of the dielectric core r_1 may vary, since we aim to investigate in which way the value of this parameter influences the profiles of the absorption spectra. We also consider the polarization of the external field to be oriented in parallel to the symmetry axis of the nanosystem z , which means that $s_a = 2$.

In Figure 2a,b, we present the absorption spectra of the SQD and the MNS, respectively, as a function of the detuning energy of the weak probe field $\hbar\delta$, for interparticle distances $R = 12.5$ nm (turquoise solid curve), 14 nm (purple dashed curve), 17 nm (pink dotted curved), and 100 nm (green dashed-dotted curve). The radius of the dielectric core is $r_1 = 6.5$ nm and its dielectric constant is $\epsilon_c = 1$. In Figure 3a,b, we present the spectra of the absorption coefficients for $\epsilon_c = 8$.

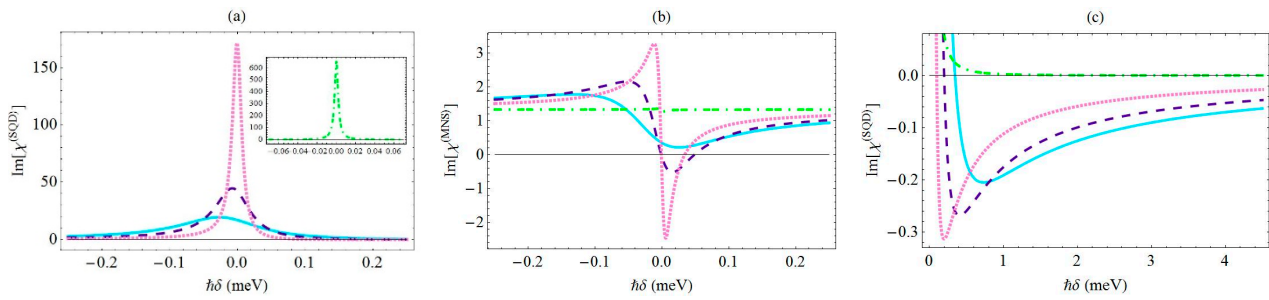


Figure 2. The imaginary part of the linear optical susceptibility of the SQD and the MNS, (a,b), as a function of the detuning energy $\hbar\delta$ of the incident field, for various center-to-center distances: $R = 12.5$ nm (turquoise solid curve), 14 nm (purple dashed curve), 17 nm (pink dotted curve), and 100 nm (green dashed-dotted curve). (c) displays gain without population inversion on the profile of the SQD absorption spectrum, within a specific range of frequencies. The rest of the physical parameters are $r_2 = 7.5$ nm, $r_1 = 6.5$ nm, $\mu = 0.65q_e$, $\epsilon_s = 6$, $T_2 = 0.3$ ps, and $\epsilon_{env} = \epsilon_c = 1$.

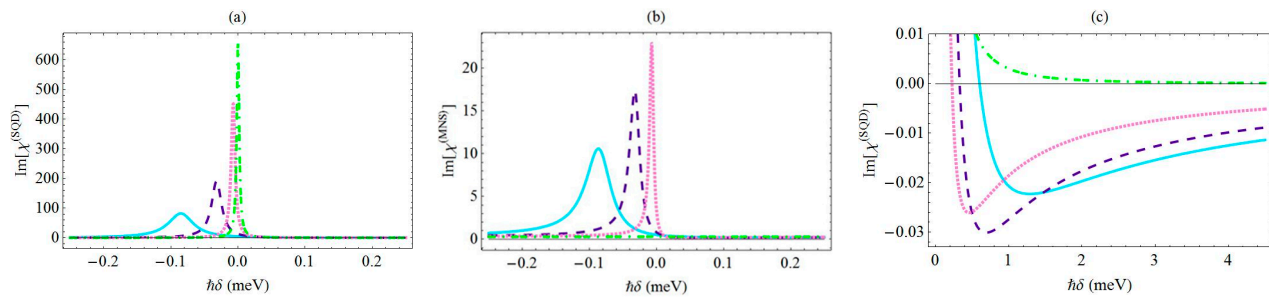


Figure 3. The linear absorption spectra of the SQD and the MNS (a,b) for various center-to-center distances (turquoise solid curve: 12.5 nm, purple dashed curve: 14 nm, pink dotted curve: 17 nm, and green dashed-dotted curve: 100 nm), with $\epsilon_c = 8\epsilon_0$. (c) displays gain without population inversion on the profile of the SQD absorption spectrum, within a specific range of frequencies. The rest of the physical parameters take the same values as in Figure 2.

4. Discussion and Conclusions

In Figure 2a, we note that the spectrum of $\text{Im}[\chi_{\text{SQD}}]$ manifests a Lorentzian-type absorption resonance. As the interparticle distance is reduced, we note that the FWHM of the absorption peak is substantially increased and its position is shifted towards negative values of detuning (Equation (5)) which are, respectively, related to the shrunk lifetime of the hybrid exciton and its red-shifted energy. At the same time, the magnitude of the absorption peak (Equation (4)) is importantly quenched. These effects owe their presence to the decrease in the value of the parameters K_I^2/K_R^2 and G_I . The emergence of gain without population inversion within a specific range of frequencies on the profile of the SQD absorption spectrum (Figure 2c) is predicted mathematically by Equation (4); according to this equation, for any set of physical parameters, $\text{Im}[\chi_{\text{SQD}}]$ is always negative, due to the negative sign of the Q constant. For intermediate values of R, the magnitude of the gain is maximized, while in the limiting case where the SQD does not practically interact with the MNS (green dotted-dashed curve: $R = 100$ nm), the profile of the absorption resonance becomes highly symmetric and the gain region is extinguished, since $M_I \rightarrow 0$. In this last case, $\text{Im}[\chi_{\text{SQD}}]_{\text{max}}$ converges to the values $-\frac{Q}{\epsilon_{\text{effs}}}$ and $\text{Im}[\chi_{\text{SQD}}]_{\text{min}} \rightarrow 0$. As seen in Figure 2b, the absorption spectrum for the MNS has a Fano-type profile for low and intermediate values of the interparticle distance. We also observe a rise in a gain region on the $\text{Im}[\chi_{\text{MNS}}]$ spectrum, the magnitude of which is maximized for an intermediate value of the center-to-center distance. In addition, for high values of the interparticle distance ($R = 100$ nm), the MNS does not interact with the SQD, and the second term of Equation (6) is extinguished, the reason being that the M_I variable converges to zero, since it is inversely proportional to the third order of R. Thus, the value of the imaginary part of χ_{MNS} is

determined by the first term of Equation (6), which is a constant. The corresponding spectral profile is a horizontal line (green dashed-dotted curve).

By comparing Figure 2a with Figure 3a, and Figure 2c with Figure 3c, we observe that the increase in ϵ_c is responsible for the enhancement and the narrowing of the absorption resonance, as well as for the gain suppression. The increase in ϵ_c leads to a decrease in G_I . As a result, the denominator of Equation (4) decreases, thus leading to the enhancement of the absorption peak. We also find that a substantial modification of the exciton's lifetime is governed by the dielectric constant of the core, since the increase in ϵ_c leads to a reduction in the FWHM of the absorption resonance. This effect can be understood in terms of Equation (5), where we note that the FWHM is proportional to the imaginary part of the self-interaction constant, G_I , the value of which decreases as we increase the dielectric constant of the core ϵ_c . The magnitude of the gain dip manifests a notable suppression, as the dielectric constant of the core is amplified (Figures 2c and 3c). The dielectric constant of the core's material also plays an important role in the absorption spectrum of the MNS. As we increase the value of the core's dielectric constant, the magnitude of the gain dip of the MNS absorption spectrum is suppressed, and above a specific value of the dielectric constant ϵ_c , the gain region is extinguished. The spectral profile of the MNS absorption coefficient strongly resembles the Lorentzian-type absorption spectrum of the SQD, in opposition to the case with $\epsilon_c = 1$ presented in Figure 2b, where it exhibits a Fano-type line shape. This is due to the fact that the increase in the value of ϵ_c causes a substantial decrease in the \tilde{M}_I factor that is introduced in the R-dependent term of Equation (6).

Author Contributions: Conceptualization, S.G.K. and E.P.; methodology, S.G.K. and E.P.; software, A.K. and S.G.K.; validation, A.K., S.G.K., and E.P.; investigation, A.K.; writing—original draft preparation, A.K., S.G.K., and E.P.; writing—review and editing, S.G.K. and E.P.; visualization, A.K., S.G.K., and E.P.; supervision, S.G.K. and E.P.; All authors have read and agreed to the published version of the manuscript.

Funding: This research received no external funding.

Institutional Review Board Statement: Not applicable.

Informed Consent Statement: Not applicable.

Data Availability Statement: The data presented in this study are available on request from the corresponding author.

Conflicts of Interest: The authors declare no conflict of interest.

References

1. Sadeghi, S.M. The inhibition of optical excitations and enhancement of Rabi flopping in hybrid quantum dot–metallic nanoparticle systems. *Nanotechnology* **2009**, *20*, 225401. [[CrossRef](#)] [[PubMed](#)]
2. Sadeghi, S.M. Plasmonic metaresonances: Molecular resonances in quantum dot–metallic nanoparticle conjugates. *Phys. Rev. B* **2009**, *79*, 233309. [[CrossRef](#)]
3. Zhang, W.; Govorov, A.O.; Bryant, G.W. Semiconductor-metal nanoparticle molecules: Hybrid excitons and the nonlinear Fano effect. *Phys. Rev. Lett.* **2006**, *97*, 146804. [[CrossRef](#)] [[PubMed](#)]
4. Yan, J.-Y.; Zhang, W.; Duan, S.-Q.; Zhao, X.-G.; Govorov, A.O. Optical properties of coupled metal semiconductor and metal-molecule nanocrystal complexes: Role of multipole effects. *Phys. Rev. B* **2008**, *77*, 165301. [[CrossRef](#)]
5. Artuso, R.D.; Bryant, G.W. Strongly coupled quantum dot-metal nanoparticle systems: Exciton-induced transparency, discontinuous response, and suppression as driven quantum oscillator effects. *Phys. Rev. B* **2010**, *82*, 195419. [[CrossRef](#)]
6. Ko, M.-C.; Kim, N.-C.; Choe, S. II; So, G.-H.; Jang, P.-R.; Kim, Y.-J.; Kim, I.-G.; Li, J.-B. Plasmonic effect on the optical properties in a hybrid V-Type three-level quantum dot-metallic nanoparticle nanosystem. *Plasmonics* **2018**, *13*, 39–46. [[CrossRef](#)]
7. Malyshev, A.V.; Malyshev, V.A. Optical bistability and hysteresis of a hybrid metal-semiconductor nanodimer. *Phys. Rev. B* **2011**, *84*, 035314. [[CrossRef](#)]
8. Ridolfo, A.; Di Stefano, O.; Fina, N.; Saija, R.; Savasta, S. Quantum plasmonics with quantum dot-metal nanoparticle molecules: Influence of the Fano effect on photon statistics. *Phys. Rev. Lett.* **2010**, *105*, 263601. [[CrossRef](#)] [[PubMed](#)]
9. Sadeghi, S.M. Gain without inversion in hybrid quantum dot–metallic nanoparticle systems. *Nanotechnology* **2010**, *21*, 455401. [[CrossRef](#)] [[PubMed](#)]

10. Kosionis, S.G.; Terzis, A.F.; Sadeghi, S.M.; Paspalakis, E. Optical response of a quantum dot-metal nanoparticle hybrid interacting with a weak probe field. *J. Phys. Condens. Matter* **2013**, *25*, 045304. [[CrossRef](#)] [[PubMed](#)]
11. Naeimi, Z.; Mohammadzadeh, A.; Miri, M. Optical response of a hybrid system composed of a quantum dot and a core-shell nanoparticle. *JOSA B* **2019**, *36*, 2317–2324. [[CrossRef](#)]
12. Nughero, B.S.; Iskandar, A.A.; Malyshev, V.A.; Knoester, J. Plasmon-assisted two-photon absorption in a semiconductor quantum dot-metallic nanoshell composite. *Phys. Rev. B* **2020**, *102*, 045405. [[CrossRef](#)]
13. Huang, C.; Zhang, H.A. Simple derivation of the shell polarizability formula and investigation of the plasmonic behavior of aluminum nanoshells with the Mie theory. *Phys. Chem. Chem. Phys.* **2021**, *23*, 23501–23507. [[CrossRef](#)] [[PubMed](#)]
14. Johnson, P.B.; Christy, R.W. Optical constants of the noble metals. *Phys. Rev. B* **1972**, *6*, 4370. [[CrossRef](#)]
15. Chang-Hasnain, C.J.; Ku, P.-C.; Kim, J.; Chuang, S.-L. Variable optical buffer using slow light in semiconductor nanostructures. *Proc. IEEE* **2003**, *91*, 1884–1897. [[CrossRef](#)]